25th International Cryogenic Engineering Conference and the International Cryogenic Materials Conference in 2014, ICEC 25–ICMC 2014

An optimal control approach for an overall cryogenic plant under pulsed heat loads

Luis Gómez Palacín[a,*], Benjamin Bradu[a], Enrique Blanco Viñuela[a], Ryuji Maekawa[b], Michel Chalifour[b]

[a]*CERN, Genève 23, CH-1211, Switzerland*
[b]*ITER Organization, Route de Vinon-sur-Verdon, CS 90 046, 13067 St. Paul Lez Durance Cedex, France*

Abstract

This work deals with the optimal management of a cryogenic plant composed by parallel refrigeration plants, which provide supercritical helium to pulsed heat loads. First, a data reconciliation approach is proposed to estimate precisely the refrigerator variables necessary to deduce the efficiency of each refrigerator. Second, taking into account these efficiencies, an optimal operation of the system is proposed and studied. Finally, while minimizing the power consumption of the refrigerators, the control system maintains stable operation of the cryoplant under pulsed heat loads. The management of the refrigerators is carried out by an upper control layer, which balances the relative production of cooling power in each refrigerator. In addition, this upper control layer deals with the mitigation of malfunctions and faults in the system. The proposed approach has been validated using a dynamic model of the cryoplant developed with EcosimPro software, based on first principles (mass and energy balances) and thermo-hydraulic equations.
© 2014 The Authors. Published by Elsevier B.V.
Peer-review under responsibility of the organizing committee of ICEC 25-ICMC 2014.

Keywords: Cryogenics, Fusion, Modeling, Simulation, Optimal Control

1. Introduction

Future large superconducting tokamak devices, such as ITER or JT60-SA, will need large cryogenic plants to maintain a good temperature range around 4.5 K in their superconducting magnets, used to confine fusion plasma. The thermal loads induced to the three parallel cryogenic refrigerators will be pulsed, as tokamaks are producing fusion plasma in a pulsed way. In JT60-SA, the thermal load varies between 5 kW and 12 kW at 4.4 K with a period of 1 hour; whereas ITER will have a thermal load between 40 kW and 65 kW at 4.4 K with a period of 30 minutes.

To handle these pulsed heat loads and ensure safe operation of the machines, several mitigation techniques are currently being studied at different levels. First, the main heat peaks can be absorbed by toroidal field coil structures of the tokamak with 4 400 tons of weight, see Maekawa et al. (2012). Second, the operation of the magnets' supercritical

---

helium cooling loops can be optimized, to compensate the peaks and damp the thermal load seen by the cryogenic plants, see Zanino et al. (2013) and Lagier et al. (2014). Finally, optimizations of the control can also be performed at the cryoplant level (in refrigerators and in the distribution system) to compensate the remaining loads.

This paper presents the development of an optimal control approach at the cryoplant level compensating the pulsed heat loads and distributing the load on the refrigerators.

2. Methodology

To test, compare and validate different control schemes, a cryogenic simulator performs dynamic simulations of the cryoplant during the thermal load pulse sequence. The model uses a first principles approach (mass and energy balances) and consists of thousands of differential algebraic equations. It was developed in the modeling and simulation environment EcosimPro, see Vázquez et al. (2010), and a dedicated cryogenic library called CRYOLIB, see Bradu et al. (2012), which provides the main components of a cryogenic plant with the thermodynamic properties of the helium calculated using the HEPAK package, see Cryodata Inc. (1999). The CRYOLIB library allows the dynamic study of the system, and calculates the evolution of the different variables, depending on the parameterization of the units, the control logic and the inputs of the system.

A previous study has been performed with this dynamic simulator to develop the basic refrigerator internal control loops and the management of the high-pressure set-point on each of the three refrigerators, see Booth et al. (2012). This simulator is re-used here to develop an additional control at a higher level. Figure 1 presents the flow diagram of the system. The supercritical helium is provided by the three refrigerators (dotted squares), collected and distributed to the five clients (in the various tokamak magnet structures). The heat loads of the clients cause the evaporation of the helium in Auxiliary Cold-Boxes (ACB), then the helium is collected and sent back to the three refrigerators. Liquid helium can also be stored or retrieved in an external Dewar during the pulses as a function of the refrigerators operation needs, see Kalinin et al. (2006) and Henry et al. (2007).
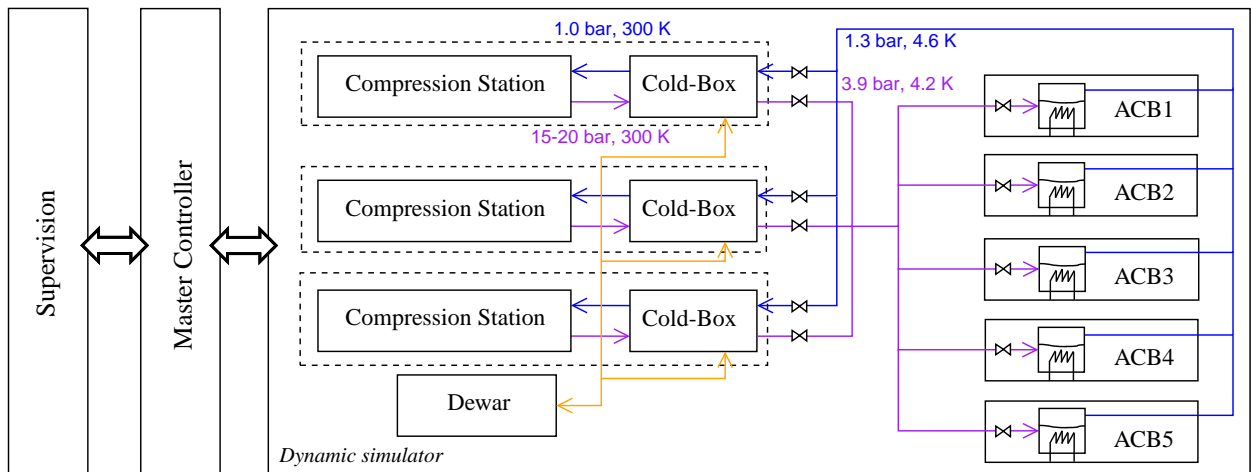

Fig. 1. Flow diagram of the cryogenic system.

To optimize the overall cryogenic system, the efficiency of each refrigerator needs to be estimated. Although the calculation of the efficiency is not direct, it may be inferred from an exergy (*B*) balance for each refrigerator, see Claudet et al. (2009, 2012):

$$B_r = \sum_{j=1}^{N} \dot{m} \cdot \left(-T_{ref} \cdot (s_{in} - s_{out}) + (h_{in} - h_{out}) \right) \tag{1}$$

where B_r is the exergy flow of each cryoplant (kW), $\dot{m}$ is the mass flow of the different input and output streams (kg/s), T_{ref} is the reference temperature (K), s is the specific entropy of each stream ($kJ/(K \cdot kg)$), h is the specific

enthalpy of each stream (kJ/kg), r is the different refrigerators ($r = 1, 2, 3$), j is the different input and output streams of each refrigerator, and N is the number of streams. The specific entropies and enthalpies are computed depending on the operating point (temperature and pressure) of each stream, while the mass flows can be obtained either by a sensor if available or by the flow equation of the corresponding valve.

3. Data reconciliation

This section describes the data reconciliation approach, which is used to estimate the measurement errors. The measurement of a process variable through a sensor includes uncertainties. The measured value ($\hat{y}$) and its actual value (y) may differ due to sensor errors. This uncertainty should be corrected in order to obtain reliable data to compute the exergy of each refrigerator. The actual value of the corresponding variable, is assumed to be proportional to the measured value, as seen in equation (2).

$$y = a \cdot \hat{y} + b \tag{2}$$

where $\hat{y}$ is the measured value, a and b are empirical parameters, which should be estimated for each sensor, and y is the real value. Basically, the data reconciliation consists in solving an optimization problem, calculating the parameters a and b and minimizing a certain objective function (J_D), which penalizes the errors in the measurement, as seen in equation (3):

$$\min_{a_i, b_i} J_D = \sum_{i=1}^{S} \beta_i \cdot \frac{(y_i - \hat{y}_i)^2}{\xi_i} \tag{3}$$

where i is the different sensors, and S is the number of sensors.

Since the different variables may have different units and ranges, the sum of the different errors are weighted according to the range of the corresponding sensor (ξ_i). In addition, the accuracy of each sensor is taken into account by the parameters β_i, which are fixed by the user. The optimization problem consists in computing the parameters a_i and b_i, which bring closer the measured and calculated variables, and fulfill the corresponding mass and energy balances. It may be easily solved using any nonlinear programming (NLP) optimization method, such as the sequential quadratic programming (SQP) methods, see Fletcher (2013). The data reconciliation can be carried out in the upper layer of the control system (supervision), and applied before each new running campaign. This approach may be applied to any section of the cryoplant. In the case of one ACB, the measured variables with uncertainties are the input mass flow ($\hat{\dot{m}}_{in}$), the output mass flow ($\hat{\dot{m}}_{out}$), and the helium level of the phase separator ($\hat{L}$), as seen in equation (4):

$$\dot{m}_{in} = a_1 \cdot \hat{\dot{m}}_{in} + b_1 \qquad \dot{m}_{out} = a_2 \cdot \hat{\dot{m}}_{out} + b_2 \qquad L = a_3 \cdot \hat{L} + b_3 \tag{4}$$

The data reconciliation infers the value of the parameters a_i and b_i, which are the solution of the minimization of the objective function (J_D). Mathematically, this may be written as:

$$\min_{a,b} J_D = \beta_{\dot{m}_{in}} \cdot \frac{(\dot{m}_{in} - \hat{\dot{m}}_{in})^2}{\xi_{\dot{m}_{in}}} + \beta_{\dot{m}_{out}} \cdot \frac{(\dot{m}_{out} - \hat{\dot{m}}_{out})^2}{\xi_{\dot{m}_{out}}} + \beta_L \cdot \frac{(L - \hat{L})^2}{\xi_L} \tag{5}$$

taking into account the mass balance for the ACB, as follows:

$$\int_{t_1}^{t_2} (\dot{m}_{in} - \dot{m}_{out}) \cdot d\tau = \left(L(t_2) \cdot \rho(t_2) - L(t_1) \cdot \rho(t_1) \right) \cdot 0.01 \cdot V \tag{6}$$

where V is the volume of the phase separator (m^3), $L(t_1)$ and $L(t_2)$ is the helium level at initial and final time (%), and $\rho(t_1)$ and $\rho(t_2)$ the helium density at initial and final time (kg/m^3).

Figure 2 shows an example of the data reconciliation for the ACB1, where the behavior of the input and output flows are represented over two cycles. The continuous lines present the measured behavior of the different variables for the first cycle, while the dotted lines presents the reconciled values for the second cycle.
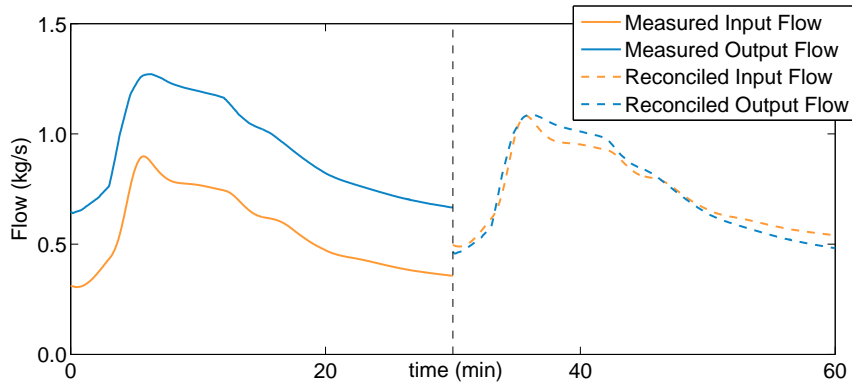
Fig. 2. Data reconciliation for ACB mass flows. The data reconciliation is carried out at the end of the first cycle (vertical line).

4. Optimal control approach

The efficiency of the three refrigerators may be different. In the cryoplant simulator, this could be modeled by different methods: 1) changing the efficiency of the turbines of the three Cold-Boxes; 2) changing the heat coefficient of the heat exchangers of the three Cold-Boxes; 3) changing the size of the valves that connect the three refrigerators with the helium distribution system, in order to reflect different pressure losses for each refrigerator.

Although the three refrigerators have different efficiencies, the cryoplant is stable as the differences between the refrigerators are compensated by the distribution system. The refrigerator with the lowest efficiency will have a larger liquid helium consumption than the others, while providing a lower cooling power; and the overall system will not operate at the optimal working point.

To solve this issue, a *master controller* has been developed to manage the power distribution among the three refrigerators. After each pulse cycle, the master controller calculates the total equivalent energy (E in kJ) provided by each refrigerator, and inferred from the exergy balance of each refrigerator. Then, the master controller compares the energy provided by each refrigerator (E_r) with the average energy ($\bar{E}$). In the following cycle, the master controller will increase the production of cooling power in the most efficient refrigerator and decreases the production of the worst ones.
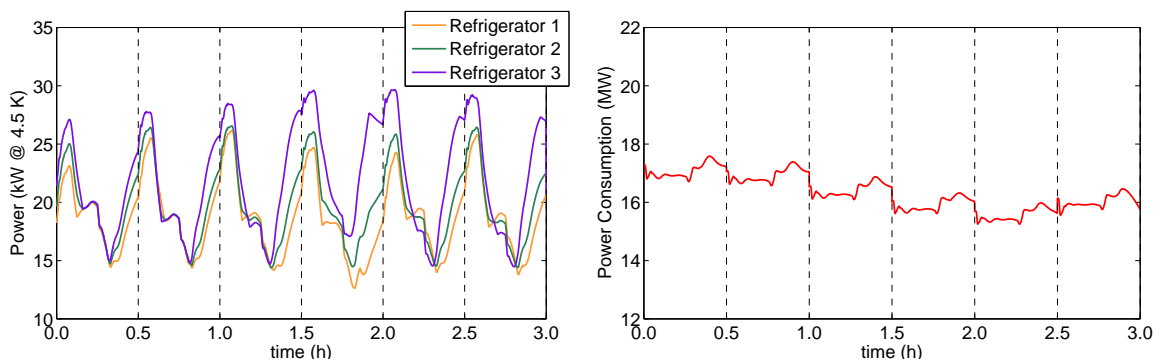

Fig. 3. Evolution of the refrigeration power provided by the three refrigerators and the total power consumption of the cryoplant, over 6 cycles; showing overall reduction in power consumption (around 7%), as desired. The dotted lines symbolize the ending of each cycle.

The manipulated variables of the master controller are the position of the valves that connect the refrigerators and the clients, see figure 1. The value of the valves positions for the cycle (k) are calculated at the initial time of the cycle, depending on the cycle ($k-1$), and kept constant during the following cycle. Equation (7) shows these variables calculation, where the valve openings are expressed as increments with respect to the initial/nominal values (Δu).

$$\Delta u_r(k+1) = \Delta u_r(k) + K \cdot (E_r(k) - \bar{E}(k)) \tag{7}$$

where k symbolizes the cycle, r symbolizes the refrigerator and K is a user parameter, which weights the smoothness of the actions of the master controller.

When the master controller modifies the state of one refrigerator, away from the nominal point, the disturbances of the different variables may get worse. When one refrigerator is far enough from its nominal value, some constraints of the cryoplant cannot be fulfilled anymore. In order to consider this, the master controller checks all the constraints of the system during each cycle. When one variable is close to the operational boundaries of the system, the master controller steps back to its previous operating point. Therefore, the parameter K should be fixed appropriately to have a smooth operation of the system. The operation of the cryoplant is shown in figure 3 where the behavior of the equivalent powers provided by the three refrigerators are represented together with the corresponding power consumption. The simulations show that as expected the master controller assigns additional cooling power to the most efficient refrigerator and consequently that the total energy consumption is lower, while respecting all cryoplants constraints, such as clients temperatures and pressures. In the current scenario, the decrease of the power consumption using the master controller is around 7%, as seen in the right hand picture of figure 3.

5. Fault management

If one equipment, such as a compressor or a turbine, is failing, the master controller should also be able to keep the cryoplant operational, while minimizing, as much as possible, the unwanted effects of the corresponding malfunction. To do so, when the fault occurs, the master controller regulates the connection valves of the refrigerators and manipulates the supply/return valves to the ACBs. The appropriate evolution of the valves depends on the corresponding fault, and may be calculated by solving an optimization problem, which penalizes the unfulfillment of the constraints, as seen in equation (8):

$$\min_{\Delta u_r(w)} J_F = \sum_{i=1}^{M} \beta_i \cdot \int_{t_1}^{t_2} \left(\max(y_i(\tau) - \gamma_{max\,i}, 0)^2 + \max(\gamma_{min\,i} - y_i(\tau), 0)^2 \right) \cdot d\tau \tag{8}$$

where $\Delta u_r(w)$ is the optimal opening/closing speed of the valves to reduce the impact on the operation, and is expressed as increments with respect to the nominal point, β_i are weight factors, y_i is the controlled variable, $\gamma_{max\,i}$ and $\gamma_{min\,i}$ are the maximum/minimum constraints, as seen in equation (9), w is the changes of the valve position, i is the different variables, and M is the number of controlled variables.

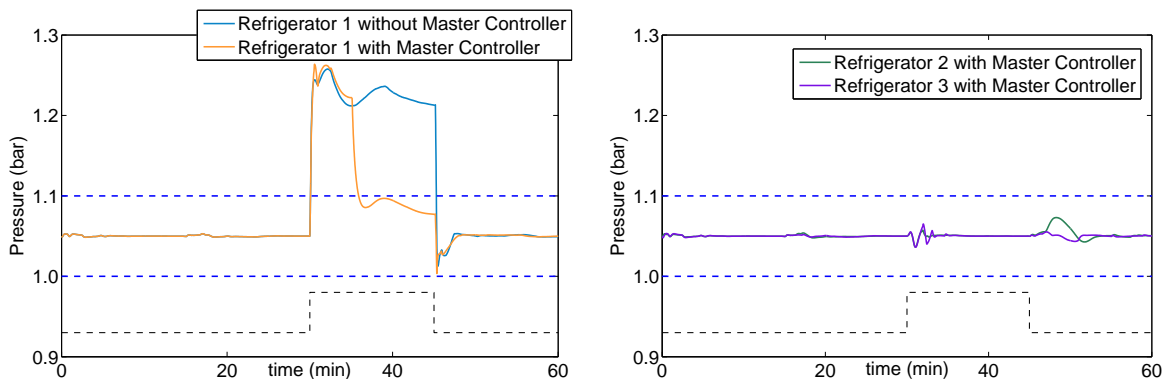$$y_i \leq \gamma_{max\,i} \qquad y_i \geq \gamma_{min\,i} \tag{9}$$

Fig. 4. Behavior of the low pressure when a sudden stop of one compressor (in refrigerator 1) takes place, with/without fault tolerance operation. The blue lines are the constraints, while the black dotted line symbolizes the time instant when the compressor is stopped.

The solution of equation (8) depends on the state of the system, and should be done off-line in the upper layer of the control system (supervision). Once the optimal opening/closing speed of the valves is calculated, it may be included into the lower-layer controller. Figure 4 shows the behavior of the low pressure (LP) of one refrigerator over two cycles. At time 30 min, one of the compressors stops, which causes the increase of the operating pressure. The yellow line shows the evolution of the system without any action from the master controller. As it can be seen, the LP goes beyond the constraints (dotted lines). The blue line corresponds to the evolution of the same variable, using fault tolerance operation. Although the operating pressure goes also beyond the limits, it is corrected after a certain time, and the constraint is fulfilled over the rest of the simulated time.

6. Conclusion

This paper describes one possible optimal operation of a cryo-system, consisting of three refrigerators in parallel, which provides supercritical helium to five clients. The total amount of supercritical helium is fixed by the cooling power demand of the clients, however the partial cooling power provided by each refrigerator may vary. Since the efficiency of the refrigerators may differ, it is a good practice to maximize the production of cooling power based on the performance of the best refrigerator and vice versa.

The cryoplant control can be done at several levels and at different time scales. First, the fast basic control loops ensure the internal refrigerator constraints in real-time. Second, the refrigerator high-pressure set-point is computed to ensure a sufficient cooling power, and a constant helium storage (in the gaseous helium storages and liquid helium tanks), as described in Booth et al. (2012). Then, additional control schemes have been presented to perform the load balancing among the refrigerators:

- Data reconciliation algorithms are executed before each new running campaign.
- Optimal balancing among the refrigerators based on the exergy balance is executed at the end of each pulse.
- Fault detection system re-equilibrates the load over the refrigerators in real-time.

These different techniques can be then modulated and implemented according to the considered system.

ITER disclaimer

The views and opinions expressed herein do not necessarily reflect those of the ITER organization.

References

Booth, W., Bradu, B., Viñuela, E.B., Gayet, P., Maekawa, R., Serio, L., Chang, H.S., Chalifour, M., 2012. Dynamic simulation of the ITER helium cryogenic system under pulsed heat loads, in: 24th International Cryogenic Engineering Conference, Fukuoka, Japan.

Bradu, B., Avezuela, R., Viñuela, E.B., Cobas, P., Gayet, P., Veleiro, A., 2012. CRYOLIB: a commercial library for modelling and simulation of cryogenic processes with EcosimPro, in: 24th International Cryogenic Engineering Conference, Fukuoka, Japan.

Claudet, S., Brodzinski, K., Ferlin, G., Lebrun, P., Tavian, L., Wagner, U., 2012. Energy efficiency of large cryogenic systems: the LHC case and beyond, in: 24th International Cryogenic Engineering Conference, Fukuoka, Japan.

Claudet, S., Lebrun, P., Tavian, L., Wagner, U., 2009. Exergy analysis of the cryogenic helium distribution system for the Large Hadron Collider (LHC), in: Cyrogenic Engineering Conference, Tucson, AR, USA.

Cryodata Inc., 1999. HEPAK 3.4. Louisville, Colorado, USA.

Fletcher, R., 2013. Practical Methods of Optimization. Wiley.

Henry, D., Journeaux, J., Roussel, P., Michel, F., Poncet, J., Girard, A., Kalinin, V., Chesny, P., 2007. Analysis of the ITER cryoplant operational modes. Fusion Engineering and Design 82, 1454–1459.

Kalinin, V., Tada, E., Millet, F., Shatil, N., 2006. ITER cryogenic system. Fusion Engineering and Design 81, 2589–2592.

Lagier, B., Hoa, C., Rousset, B., 2014. Validation of EcosimPro model for assessing 2 heat load smoothing strategies on HELIOS experiment. Cryogenics 62, 60–70.

Maekawa, R., Takami, S., Oba, K., Iwamoto, A., Chang, H., Forgeas, A., Chalifour, M., Serio, L., 2012. Investigation of mitigation technique for the ITER TF structure cooling circuits, in: 24th International Cryogenic Engineering Conference, Fukuoka, Japan.

Vázquez, F., Jiménez, J., Garrido, J., Belmonte, A., 2010. Introduction to Modelling and Simulation with EcosimPro. Pearson.

Zanino, R., Bonifetto, R., Hoa, C., Richard, L.S., 2013. 4C modeling of pulsed-load smoothing in the HELIOS facility using a controlled bypass valve. Cryogenics 57, 31–44.